An Ultra-wideband Off-axis Reflector Lens

1st Mingyan Zhong
University of Glasguw
Centre for Advanced Electronics (CAE)
Glasgow, UK
m.zhong.1@research.gla.ac.uk

2nd Yunan Jiang
University of Glasguw
Centre for Advanced Electronics (CAE)
Glasgow, UK
2602587j@student.gla.ac.uk

3rd Yufei Ma
University of Glasgow
Centre for Advanced Electronics (CAE)
Glasgow, UK
y.ma.1@research.gla.ac.uk

line 1: 4th Chong Li
University of Glasgow
Centre for Advanced Electronics (CAE)
Glasgow, UK
chong.li@glasgow.ac.uk

***Abstract*— The paper describes the design, fabrication and characterization of an ultra-wideband off-axis reflector lens operating between 6.8 GHz and 16.8 GHz. The lens is constructed using a single layer metasurface, consisting of a single ring with two equal openings. The design achieves an efficiency greater than 80% polarization conversion and a cross-polarization gain of 10 dB at the center frequency. The experimental results are in good agreement with the numerical simulations.**

Keywords*— *ultra wideband, reflector lens, metasurface

I. Introduction

Microwave and optical lenses play a crucial role in manipulating the propagation of electromagnetic waves across various applications, including communication, imaging, and sensing. Polarization is a key property of electromagnetic waves and traditional techniques such as optical activity of crystals and the Faraday Effect have been employed for polarization manipulation, but they are constrained by limitations related to bandwidth and size [1]. Metamaterials, artificially engineered structures, offer a promising platform for achieving precise control over polarization due to their distinct advantages such as minimal thickness and low losses [1-3]. However, metamaterials are often restricted to narrow bandwidths [4-6].

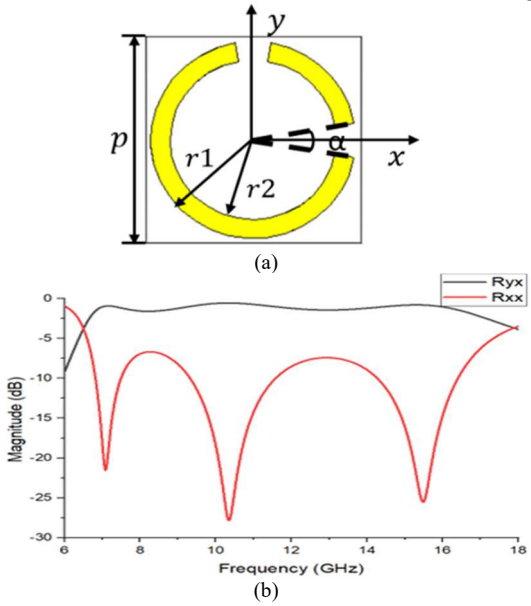

Fig. 1. (a) The proposed SRR unit. p = 7 mm, r1 = 3 mm, r2 = 2 mm, α is the opening angle. (b) The simulated of cross-polarized reflection Rxy and co-polarized reflection Rxx (α = 30°).

This paper presents a high-efficiency, ultra-broadband reflection-mode metasurface polarizer that operates in the frequency range between 6.8 GHz and 16.8 GHz. The proposed polarizer has unit cells consisting of single layer of metal rings with a double-split configuration. The rings are fabricated on a substrate backed by a metal layer on the other side. By rotating the opening angles and orientation of the splits, the reflection phase shift of 2π can be achieved. We have taken advantage of this property and develop a microwave lens that shows wide bandwidth and high gain.

II. Desgin and Simulation

Fig. 1(a) presents the top view of the unit cell of the polarizer, which consists of a double-split metallic ring on a metal backed substrate. By adjusting the opening angle of these two splits, the polarizer can achieve a 180-degree phase shift while changing the polarization of the incident wave by 90 degree. Fig. 1 (b) shows three primary resonant modes at frequencies of 7.08 GHz, 10.36 GHz, and 15.5 GHz appear when an x-polarized wave impinges on the surface. These resonant modes noticeably transform the incident wave into cross-polarized output, resulting in a broadband conversion range spanning over 10 GHz, from 6.8 GHz to 16.8 GHz. Within this operational frequency band, the conversion rate exceeds 80%. Notably, the unit's identical configuration along both the x and y directions facilitates polarization conversion for both x and y-polarized incident waves. Additionally, circularly polarized waves can be decomposed into their x and y components, and the reflection will also switch to the opposite circular polarization e.g., from right-circular polarization (RCP) to left-circular polarization (LCP) or vice versa.

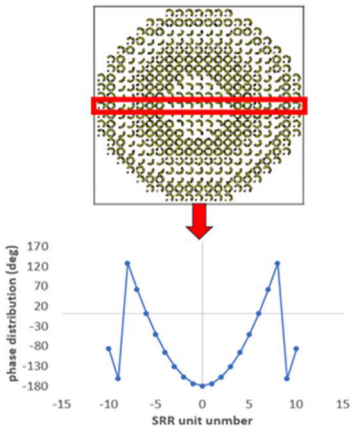

Fig. 2. Illustration of the full lens and the meta cells showing phase change over 180º.

Lens design formula is based on [7] is as follows.

$$\Delta\varphi = \frac{2\pi}{\lambda}\left(\sqrt{F^2 + (md)^2} - F\right) \quad (1)$$

where λ represents the operating wavelength, while d denotes the length of the unit cell. m = 0, 1, 2, … the index number of the cells, corresponds to the cell's position from the central one to the left and right. The focus length is denoted by F. Achieving a phase difference of 0°-180° is accomplished by adjusting the opening angle of the split-ring resonator (SRR). For phase differences between 180° and 360°, the SRRs with a 0°-180° phase difference can be rotated by 90°.

To showcase the lens's focusing capability, we designed an off-axis lens with F = 70 mm and d = 7 mm. The complete structure of the metasurface lens is illustrated in Fig. 2.

The lens was modelled and simulated using the time domain solver in CST Studio Suite software. Fig. 3((a)) (b) displays shows the a 2D cross-sectional view of power distribution when a at 10 GHz plane wave is incident onto the lens from the top and Fig.3 (b) shows the focal point of the lens at 7 cm above the lens. The proposed lens Fig. 3 (c) exhibits a gain of over 10 dB at 10 GHz , as depicted in Fig. 3(c), indicating a reasonably high focusing capability efficiency. Additionally, considering it is difficult to characterise the lens once the incident and reflected lens are aligned, we designed an off-axis lens as shown in the Fig 3 (d) demonstrate the lens's off-axis focusing capability, also showing . good focusing capability. Other frequency points were also simulated and it was noticed that due to the different wavelengths of the incident waves at various frequency points, slight variations in the focus length are observed. The maximum power concentration occurs around 7 cm at 10 GHz, which aligns with the designed focal length. The proposed lens exhibits a gain of over 10 dB at 10 GHz, as depicted in Fig. 3(c), indicating a reasonably high efficiency.

III. Fabrication and Experimental Result

The proposed lens was fabricated on an FR-4 substrate that has a dielectric constant of 4.3. The thicknesses of the substrate and the copper are 2.4 mm and 1 oz (35 µm), respectively and the overall area of the lens is 15 cm *15 cm that is equivalent of 21*21 meta cells.

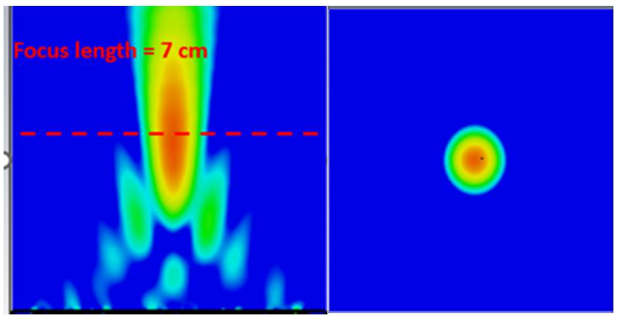

(a) (b)

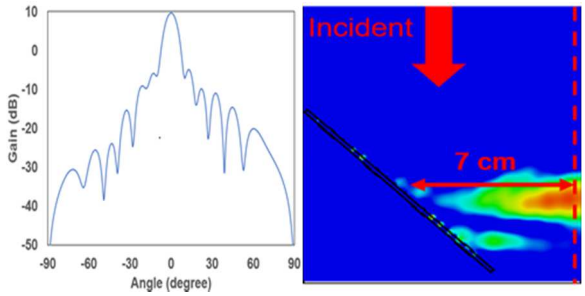

(c) (d)

Fig. 3. (a) Cross-sectional view of the focused beam; (b) top-view of the focal point at 7 cm away from the lens (c) The cross-polarized gain at 10 GHz. (d) The simulated beam with a lens tilted by 45º.

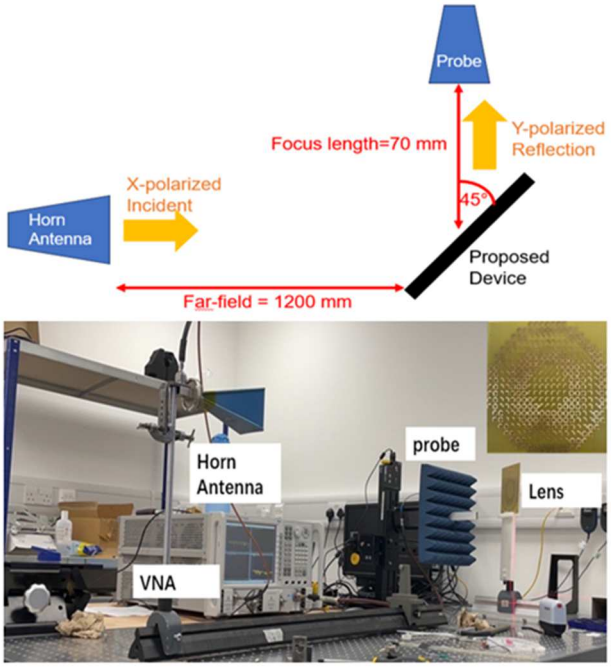

Fig. 4. Measurement setup and schematic showing an X-band horn antenna as a transmit antenna on the left and a waveguide antenna as a probe on the right. The inset shows the fabricated lens.

Fig. 4 illustrates the measurement setup employed for testing the metasurface lens. An X-band square gain horn antenna (Gain=10 dBi) and an open-ended waveguide were used as the source and the probe, respectively, operating within the frequency range of 8.2 GHz to 12.4 GHz. Note that the frequency limitation of the source and probe antennas prevented us from exploring the full operating bandwidth of the proposed lens. The source antenna was placed on a fixed post, while the probe antenna was mounted on a motorized two-dimensional linear scanning system equipped with high-precision translation stages (+/- 5 µm accuracy) for horizontal and vertical scanning. The lens, rotated at a 45-degree angle, was placed approximately 1200 mm away from the source antenna in its far-field zone to ensure a plane wave incident onto the lens. Microwave absorbers were attached to the base of the probe antenna and the translation stages to prevent reflections. A Keysight E8361A vector network analyzer (VNA) was calibrated using the SOLT method with Keysight's 85052D calibration kits for the frequencies ranging from 10 MHz to 18 GHz, despite the

antennas' cut-off frequencies. A LabVIEW program was developed to control the translation stages and the VNA [8].

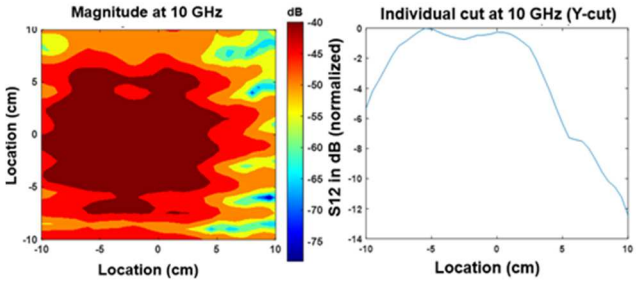

Fig. 5. Measurement of the reference plane without the presence of the lens showing (left) Power distribution (right) Normalized gain of the transmit antenna.

The electric field distribution of the horn antenna at the reference plane where the lens sat was first measured with the test system and the results are depicted in Fig. 5, showing uniform distribution of magnitude of the transmit antenna.

Fig. 6, Fig. 7, and Fig. 8 depict the electric fields measured at a distance of 2.5 cm from the center of the lens, at frequencies of 8 GHz, 10 GHz, and 12 GHz, respectively. The lens, when rotated by a 45-degree angle, exhibits an approximate gain of 10 dB higher than the reference plane of the horn antenna within the frequency range of 8 GHz to 12 GHz. However, both the simulation and measurement results indicate the presence of a relatively high-gain side lobe adjacent to the main lobe. This occurrence arises due to the phase difference resulting from the lens declination. In scenarios involving high-frequency bands like the Terahertz range, where the wavelength is considerably short, the phase difference caused by lens rotation cannot be underestimated. Therefore, the design should incorporate corresponding phase compensation techniques to enhance the gain at the focus. Remarkably, the measured results align well with the numerical simulations.

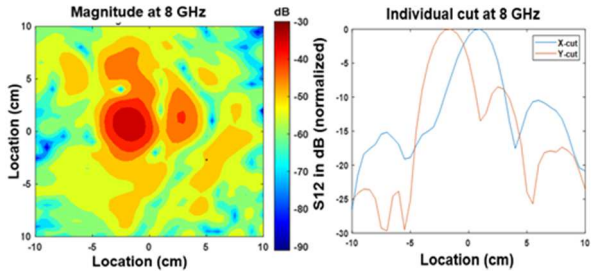

Fig. 6. (a) The electric field in dB and (b) the normalized gains of the X-cut and Y-cut of the lens at 8 GHz.

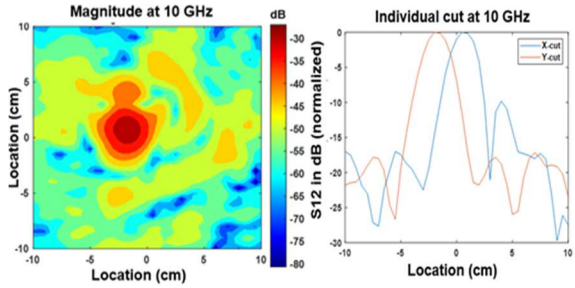

Fig. 7. (a) The electric field in dB and (b) the normalized gains of the X-cut and Y-cut of the lens at 10 GHz.

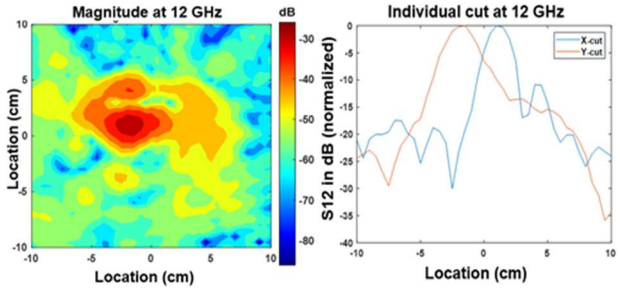

Fig. 8. (a) The electric field in dB and (b) the normalized gains of the X-cut and Y-cut of the lens at 12 GHz.

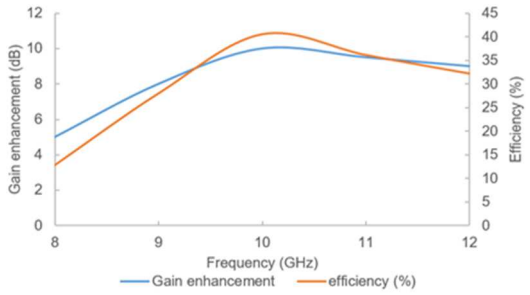

Fig. 9. Measured gain enhancement and efficiency from 8-12 GHz

Comparing the gain of the standard horn antenna (10dBi), According to Fig 89. shows, there are indicated remarkable gain enhancements with the proposed device across 8 GHz to 12 GHz and . The max gain enhancement and efficiency can reach around 10 dB and 40% at the center frequency 10 GHz,. where $Efficiency = (\frac{\lambda}{\pi} * \mathrm{D})^2 * 10^{G/10}$, G is Gain in dB, and D is dimension of the device.

IV. Conclusion

This paper has presented the design, simulation, fabrication, and testing of a high efficiency ultrabroad bandwidth reflection meta-surface lens operating within the frequency range of 6.8 GHz to 16.8 GHz. The proposed lens, based on multi-split single metal rings, achieves a cross-polarization gain enhancement of around 10 dB at the center frequency 10 GHz with good angular stability. The simplicity of the structure and its strong performance make this meta-surface lens an excellent platform for further research, including tunable and programmable meta-surface designs and polarizers for the Terahertz frequency range. Furthermore, in the mm-band, this type of reflection lens demonstrates strong feasibility as the reflection path can be adjusted by introducing angular declination.

Acknowledgement

This work was partially supported by the Engineering and Physical Research Council, UK (Grant No. EP/X017613/1). The authors would like to thank the staff of Electronics Workshop at James Watt School of Engineering, the University of Glasgow for fabricating the lens.

Reference

[1] M. I. Khan, Q. Fraz and F. A. Tahir, "Ultra-wideband cross polarization conversion metasurface insensitive to incidence angle," Journal of Applied Physics, vol. 121, (4), pp. 45103, 2017

[2] A. K. Azad et al, "Ultra-thin metasurface microwave flat lens for broadband applications," Applied Physics Letters, vol. 110, (22), pp. 224101-224101, 2017.

[3] Nanfang Yu et al, "Light Propagation with Phase Discontinuities: Generalized Laws of Reflection and Refraction, " Science, vol. 334, pp. 333-337, 2011.

[4] H. Chen et al, "A review of metasurfaces: physics and applications," Reports on Progress in Physics, vol. 79, (7), pp. 076401-076401, 2016.

[5] Y. Chiang and T. Yen, "A composite-metamaterial-based terahertz-wave polarization rotator with an ultrathin thickness, an excellent conversion ratio, and enhanced transmission," Applied Physics Letters, vol. 102, (1), pp. 11129, 2013.

[6] C. Xue et al., 'An Ultrathin, Low-Profile and High-Efficiency Metalens Antenna Based on Chain Huygens' Metasurface', IEEE Trans. Antennas Propag., vol. 70, no. 12, pp. 11442–11453, Dec. 2022.

[7] Z. Sun, F. Huang and Y. Fu, "Graphene-based active metasurface with more than 330° phase tunability operating at mid-infrared spectrum," Carbon (New York), vol. 173, pp. 512-520, 2021

[8] A. Al-Moathin et al., 'Characterization of a Compact Wideband Microwave Metasurface Lens for Cryogenic Applications', Apr. 04, 2023. http://eprints.gla.ac.uk/297802/ (accessed Jul. 06, 2023).